Delft University of Technology

Micro-Propulsion

AE4S07 - Project 17b

Analytical Relations for Performance Characterization of CD Micro-nozzles

Author:
Arthur, Thiam (4472586)
October 7, 2020

Instructor: Dr. A. Cervone

1 Introduction

Recent trends in the miniaturization of satellites have generated the need for the miniaturization and optimization of satellite subsystems. One of the main challenges in doing so is the ability to maintain similar performance characteristics while significantly reducing size and weight of components. The miniaturization of the propulsion system proves to be particularly difficult, due to the significant performance losses that accompany a reduction in size.

The assessment of the effects various sizing parameters have on the performance of micro-propulsion systems is most widely done through elaborate CFD simulations. These simulations can be quite accurate, but are not very suitable for preliminary sizing as they can be computationally demanding. It is therefore of interest to develop a set of analytical relations to predict the performance of a given micro-propulsion system to an acceptably accurate degree, while limiting the necessity of elaborate computational programs. The work presented in this report uses the results of several research papers to present a simplified analytic method for determining micro-nozzle performance . Recommendations are also given on how this approach can be complemented by CFD analysis to develop an accurate relation for the expected discharge coefficient.

The theory used to develop this analytic approach is first presented in section 2. section 3 discussed the implementation and results of the analytic approach applied to a micro-nozzle of similar dimensions to that analysed in [1]. Finally section 4 discussed the validity of the assumptions made in this report, and provides recommendations on how this work might be improved.

2 Literature Study

In order to characterize the performance losses of micro-nozzles, the metrics upon which to base the analysis must first be established. To this end, the performance of a nozzle according to "Ideal Rocket Theory" (IRT) is first analysed. Then, performance losses observed in CFD research of micro-nozzles is discussed, and a short literature study regarding the causes of these performance losses is presented. Finally, the 'Reference Temperature Approach' is used in combination with flat plate boundary layer theory to present a simplified approach for modelling the performance.

2.1 Ideal Performance Parameters

The ideal performance of a nozzle can be determined with IRT, provided that the nozzle shape and initial flow conditions are known. These are also the boundary conditions of the analysis, and will be determined in more detail in section 3. First, the mass flow through the nozzle can be determined with [3]:

$$\mathrm{m} = \frac{\Gamma \cdot \mathrm{p_c} \cdot \mathrm{A_t}}{\sqrt{\mathrm{R} \cdot \mathrm{T_c}}} \tag{1}$$

Where subscripts 'c' and 't' denote combustion chamber and throat conditions respectively. The vanderkerckhove function Γ is given by [3]:

$$\Gamma = \sqrt{\gamma} \cdot \left(\frac{2}{\gamma+1}\right)^{\left(\frac{\gamma+1}{2(\gamma-1)}\right)} \tag{2}$$

Where γ is the gas specific heat ratio. Once the massflow is known, the ideal thrust (assuming ideal expansion) is defined as follows [3]:

$$F_{id} = m \cdot U_{eq} = m \cdot \sqrt{2 \cdot \frac{\gamma}{\gamma-1} \cdot \frac{\mathrm{R_A}}{\mathrm{M}} \cdot \mathrm{T_c} \cdot \left(1 - \left(\frac{\mathrm{p_e}}{\mathrm{p_c}}\right)^{\left(\frac{\gamma-1}{\gamma}\right)}\right)} + (p_e - p_a) \cdot U_e \tag{3}$$

The thrust coefficient of the configuration can then be determined using the result of Equation 3 [3]:

$$C_F = \frac{F}{p_c \cdot A_t} \tag{4}$$

This set of formulas can be used as a baseline for the study. On the one hand, they will be used to determine the ideal performance of a given nozzle configuration. On the other, performance losses will be calculated from this baseline to estimate the true performance. The two can then be combined in order to compare the expected efficiency of different nozzle configurations.

2.2 Performance Losses

Research and testing has shown that nozzles never reach the ideal performance estimated by IRT. Some factors affect nozzles of all sizes, and some are specific to small nozzles. The characteristic that sets micro-nozzles apart from their larger counterparts is the fact that the boundary layer is proportionally much larger with respect to the throat diameter. The Reynolds number of the flow in a nozzle is a good measure for how large exactly this boundary layer is, and is traditionally given by [3]:

$$Re = \frac{\rho \cdot v \cdot D}{\mu} \tag{5}$$

For micro-nozzles with a non-circular cross section, the diameter D can be replaced with the hydraulic diameter D_h using [1]:

$$D_h = \frac{4A}{p} \tag{6}$$

Where A is the cross-sectional area, and p is the perimeter. As can be seen from Equation 5, smaller nozzles will naturally cause the flow Reynolds number to become very small. Where regular nozzles operate at Reynolds numbers well above 100,000, micro-nozzle Reynolds numbers can drop much lower than that. As will be discussed in the following sub-sections, this causes some performance losses to have a much more pronounced effect.

2.2.1 Divergence Loss

The first loss to reduce the performance of a nozzle is the divergence loss. Any nozzle that has an exit half angle larger than 0° will not eject gases parallel to the direction of thrust. The flow will have momentum components in directions perpendicular to the thrust vector. Because the nozzle is symmetric, these perpendicular momentum components cancel each other out and typically do not cause thrust misalignment. They do however contribute to a loss in thrust, as not all momentum is utilized to propel the spacecraft forward. The resulting loss is calculated as a factor, called the divergence thrust correction factor. It is given by [3]:

$$\epsilon_{div} = 1 - \frac{1 - cos(\alpha)}{2} \tag{7}$$

Where α is the exit half angle of the nozzle. As can be seen, this loss factor is dependent only on the exit half angle, and affects large and small nozzles to a similar degree.

2.2.2 Boundary Layer Losses

The second, and most impactful, performance losses originate from the boundary layer formed along the nozzle wall. Due to viscous flow effects, the flow travels at a slower speed close to the nozzle walls. This effectively "deflects" the full flow, and affects nozzle performance. Micro-nozzles are particularly affected by this phenomenon for two reasons:

- As will be shown, the low Reynolds number significantly increases the skin friction coefficient. This directly affects the effective flow deflection caused by the boundary layer. Low Reynolds numbers inherently cause boundary layers to grow larger.
- As a result of boundary layer growth, the effective nozzle areas are reduced. In a large nozzle, the amount by which these are reduced is insignificant in comparison to the size of the nozzle. However in micro-nozzles the relative size of a boundary layer is much larger, hence affecting performance differently.

Boundary layer characterization is perhaps the most important element in predicting performance losses for micro-nozzles, as they significantly change the effective internal geometry. In order to make an analytical performance loss prediction, a simplified model for determining boundary layer properties is necessary. For linear convergent-divergent micro-nozzles, the flat plate boundary layer solutions may be used as an approximation. section 4 discusses the validity of this assumption, and elaborates on possible improvements. According to flat plate boundary layer theory, the skin friction coefficient for incompressible, laminar flow is given by [3]:

$$c_{fx} = \frac{0.664}{\sqrt{Re_x}} \tag{8}$$

This equation explains why lower Reynolds numbers increase the skin friction coefficient. The effect of compressibility is addressed in subsection 2.3. Subsequently, the momentum thickness and displacement thickness are given by Equation 9 and Equation 10 respectively [3]:

$$\theta_x = c_{fx} \cdot x \tag{9}$$

$$\delta^* = 2.59036 \cdot \theta_x \tag{10}$$

The displacement thickness provides a measure for how much the flow is effectively "displaced" by the boundary layer. Note that for shorter wall lengths, the final displacement thickness is also lower. The angle of the nozzle divergent should therefore be selected as to optimize the balance between displacement thickness and divergence losses. The true area ratio of a nozzle can then be found using:

$$\left(\frac{A_e}{A_t}\right)_{true} = \frac{2 \cdot (R_e - \delta^*)}{W_t} \tag{11}$$

Where W_t is the throat width. It is important to note that here the throat diameter remains unchanged. The boundary layer is assumed to start developing at the throat, and increase in size until the nozzle exit. section 4 discusses the implications of this assumption. Furthermore, this boundary layer solution assumes the flow remains laminar and attached. This assumption can be made for low Reynolds number flow, as the higher flow viscosity makes turbulent flow less likely.

2.2.3 Momentum Losses

In addition to the modification of effective nozzle geometry, the presence of a boundary layer also causes momentum losses. The flow loses momentum in the boundary layer, and this has to be seperately accounted for. The thrust loss due to momentum is given by [3] as:

$$\Delta F_{momentum} = (\rho_e \cdot u_e \cdot (2\pi R_e) \cdot \theta_e) \cdot u_e \tag{12}$$

Note that the circumference term here must be replaced with the equivalent perimeter for nozzles of non-circular cross section.

2.3 Reference Temperature Approach

The approach to predicting boundary layer properties presented in the previous section is based on the assumption that the flow is incompressible. However as the flow is accelerated through the nozzle, it becomes supersonic. This means it can no longer be assumed that the flow is incompressible. [2] presents a "Reference Temperature Approach", whereby the skin friction coefficient is corrected with a factor that is based on an average temperature across the boundary layer. According to [2], such a correction can be made using:

$$c_f = c_{f,i}\left(\frac{T_w/T_0 + 1}{2} + 0.22\frac{\gamma - 1}{2}M^2\right)^{-0.6} \tag{13}$$

Where T_w is the wall temperature, and T_o is the stagnation temperature at the point where the skin friction coefficient is being determined. We consider only the exit stagnation temperature here, since the flat plate boundary layer characteristics will be determined at the exit of the nozzle to quantify the loss in exit area. The exit total temperature is determined using isentropic relations in the equation below. Note however that this equation could be used for any point along the nozzle, as long as the corresponding flow mach number is used:

$$T_{0_e} = T_e \cdot \left(1 + \frac{\gamma - 1}{2} \cdot M_e^2\right) \tag{14}$$

2.4 Aggregate Performance Loss

In order to determine the aggregate of all losses described in this chapter, a procedure for progressively implementing each loss must be determined.

The first step is to determine loss factors that are independent of boundary layer effects. The divergence thrust correction factor is thus first determined based on the divergent half angle.

Next, the boundary layer properties are determined. The compressible skin friction coefficient, exit momentum thickness and exit displacement thickness are all calculated based on known flow parameters. This allows the following steps to be taken in relation to boundary layer effects:

1. Thrust reduction due to momentum loss is determined based on momentum thickness.
2. The true area ratio is determined based on the displacement thickness.
3. This true area ratio induces a lower exit pressure than predicted by IRT. The effective pressure ratio and exit pressures are iteratively determined using [3]:

$$\frac{\mathrm{A_e}}{\mathrm{A_t}} = \frac{\Gamma}{\sqrt{\frac{2\gamma}{\gamma-1} \cdot \left(\frac{\mathrm{p_e}}{\mathrm{p_c}}\right)^{\left(\frac{2}{\gamma}\right)} \left(1 - \left(\frac{\mathrm{p_e}}{\mathrm{p_c}}\right)^{\left(\frac{\gamma-1}{\gamma}\right)}\right)}} \tag{15}$$

4. The resulting aggregate thrust loss is calculated.

The aggregate thrust loss combines the divergence loss, momentum loss and reduced exit pressure. The true thrust, as estimated by this methodology, is thus given by:

$$F_{true} = m \cdot \epsilon_{div} \cdot \sqrt{2 \cdot \frac{\gamma}{\gamma - 1} \cdot \frac{\mathrm{R_A}}{\mathrm{M}} \cdot \mathrm{T_c} \cdot \left(1 - \left(\frac{\mathrm{p_e}}{\mathrm{p_c}}\right)^{\frac{\gamma-1}{\gamma}}_{true}\right)} - \Delta F_{momentum} \tag{16}$$

The thrust coefficient can then be determined with [3]:

$$C_{F_{true}} = \frac{F_{true}}{p_c \cdot A_t} \tag{17}$$

3 Application of Analytical Relations

In order to verify the accuracy of the method presented in section 2, a basis for comparison should be selected. In [1], C. S. Ganani performs a CFD analysis to determine the performance of both converging-diverging and aerospike micro-nozzles. This chapter takes the same nozzle dimensions as a template for analysing and comparing the analytical results to the numerical results. Furthermore, a sensitivity analysis is performed to determine how certain parameters affect performance. This is used to lay out a method for identifying an optimum design, given the required constraints.

3.1 Nozzle dimensions

The following table lists the nozzle parameters relevant to the presented analytical approach:

Table 1: Nozzle parameters [1]

Parameter	**Value**	**Unit**
Throat Width	45	μm
Nozzle Depth	0.1	mm
Area Ratio	16.971	-
Exit half angle	15	$^\circ$

Here, as is explained in [1], the actual geometric area ratio is sized for an operational exit pressure of 1000 Pa . It should be noted however that the CFD simulations presented in [1] themselves were performed at an ambient pressure of 30 Pa. This is because the simulation is meant to replicate ground testing conditions, which were assumed to be executed at a different pressure than the optimum that the geometric area ratio was designed for. The only parameter that remains unidentified in the analytical approach presented above is the wall temperature. The wall temperature has a significant effect on nozzle performance, and should be more closely analysed in future research. For the time being, an average between exit flow temperature and ambient temperature of 160 K was assumed. The following table lists the resulting boundary layer and performance loss parameters that result from the described approach:

Table 2: Loss factor parameters

Parameter	**Symbol**	**Value**	**Unit**
Divergence Loss Factor	ϵ	0.983	-
Incompressible skin friction	c_{f_i}	1.36e-2	-
Compressible skin friction	c_f	7.61e-3	-
exit momentum thickness	θ_e	1.12e-5	m
exit displacement thickness	δ^*	2.91e-5	m
momentum loss thrust reduction	$\Delta F_{momentum}$	1.89e-3	mN
true area ratio	$\left(\frac{A_e}{A_t}\right)_{true}$	15.7	-
true pressure ratio	$\left(\frac{p_c}{p_e}\right)_{true}$	0.0037	-
Corrected thrust	F_{true}	2.15	mN

The results from this analysis can then compared to the equivalent ideal and numeric performances. The table below lists some of the nozzle performance parameters used to compare the three different approaches. Note that the numerical performance values were obtained from [1].

Table 3: Results Comparison

Parameter	**Ideal**	**Numerical**	**Analytical**	**Unit**
mass flow	3.09	3.14	3.09	mg/s
Thrust	2.36	2.27	2.17	mN
C_F	1.75	1.68	1.6	-
Isp	77.6	73.7	70.84	s
Throat Reynolds Number	2389.45	2860	2400	-
Thrust Efficiency	100	96.2	91.26	%
True/ideal Area Ratio	100	-	92.38	%

As can be seen, for this particular nozzle geometry, the analytical approach somewhat underestimates the nozzle performance as predicted by the numerical approach but is still relatively accurate. The following section provides more insight into how each design parameter affects the nozzle performance section 4.

3.2 Sensitivity Analysis & Design Choice

The analytical approach presented in this report is sensitive to a number of different parameters, the influence can be observed through several variables. The main parameters considered in this sensitivity analysis are the divergent half angle, the throat width and the chamber pressure. The effect of these design parameters can be observed by analyzing the resulting thrust coefficient, specific impulse, and several other losses. In order to better understand how these three design parameters affect the performance, a plotting tool was built. The tool [1] allows all three design parameters to be varied. The resulting performance curves are then plotted in multiple plots, depending on the input settings. The image below shows an example of the settings resulting in 3 plots, each for a different throat width, where each curve represents how the thrust efficiency changes as function of the exit angle for a given chamber pressure:

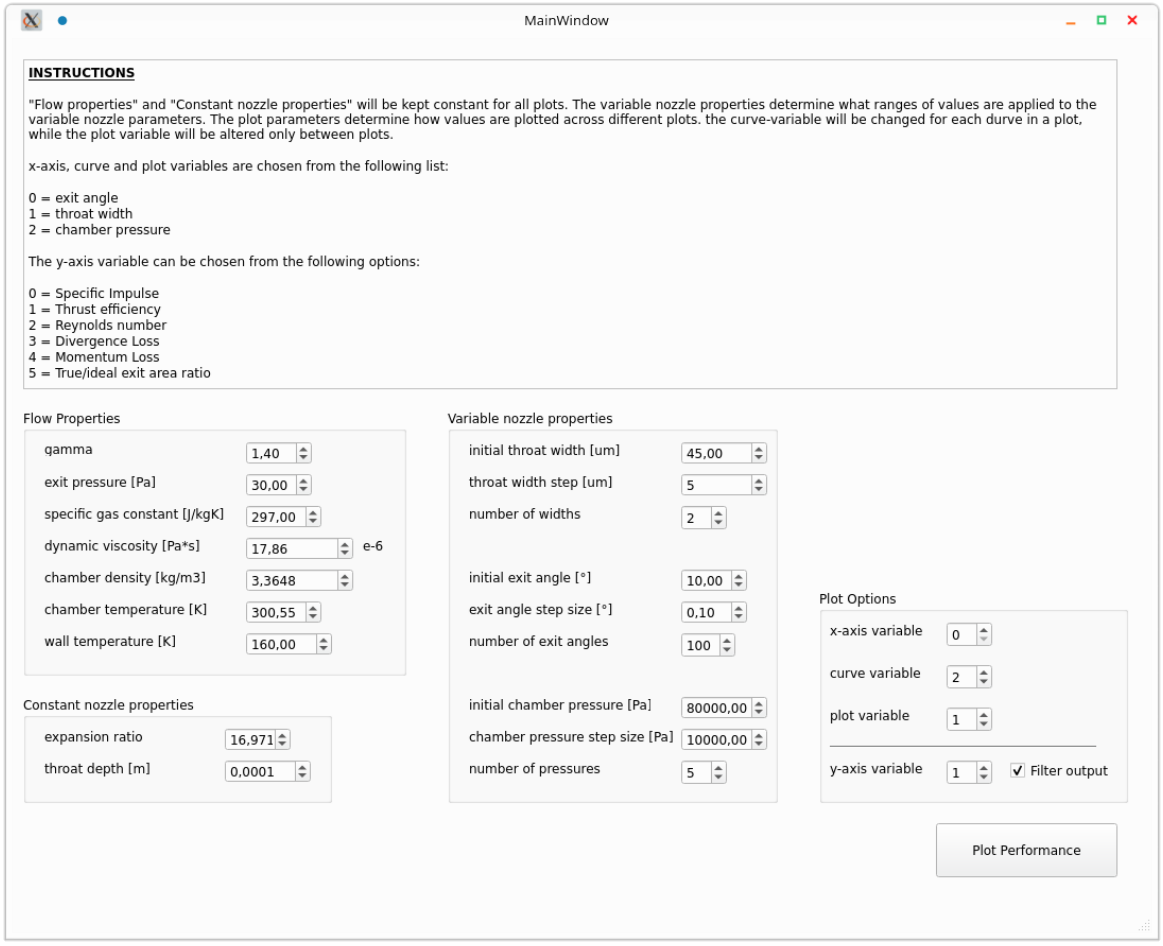

Figure 1: Settings for plots results as described above

The first resulting plot of this curve is corresponds to a throat width of $45\mu m$, and shows the variation of thrust efficiency as a function of exit angle for 10 different combustion chamber pressures, ranging from 0.8 bar to 2.6 bar. This corresponds to Reynolds numbers ranging from roughly 635 to 2070:

[1] https://github.com/ArthurThiam/Microprop-Performance

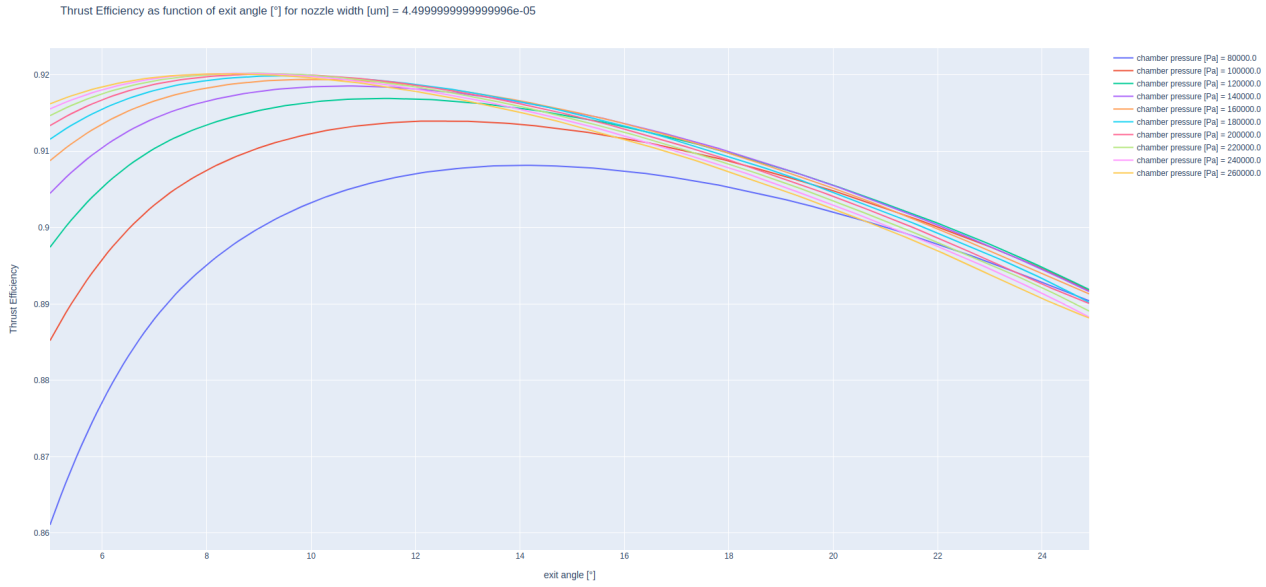

Figure 2: Thrust efficiencies as function of divergence angle

As can be deduced from this graph, the maximum thrust efficiency achievable for a given throat width increases with increasing chamber pressure. Additionally, the optimum divergent half angle to obtain this maximum thrust efficiency decreases with increasing chamber pressure. For a chamber pressure of 0.8 bar, a maximum efficiency of 0.908 is found at roughly 14.2 degrees. For a chamber pressure of 2.2 bar however, a maximum efficiency of 0.92022 is found at roughly 9 degrees. This shows that the divergent losses start outweighing the boundary layer effects much sooner for higher value of Re. In other words, a higher Reynolds number flow is less susceptible to boundary layer losses than a low Reynolds number flow. It appears that, for this specific throat width, further increasing the chamber pressure past 2.2 bar starts reducing the maximum efficiency again. This specific configuration corresponds with a Reynolds number of 1752 (as can be found by switching the y-axis variable in the settings to 2).

We can also observe how the different loss parameters change as a function of various design parameters. Plotting the true area ratio as a function of divergence angle reveals how the true exit area ratio approaches the ideal area ratio (16.97) for higher angles. This is due to the fact that lower divergence angles require longer nozzles to reach the design exit area. This gives the boundary layer more time to develop, and as a result reduces the true area ratio. The following image corresponds to the same design parameters as Figure 1:

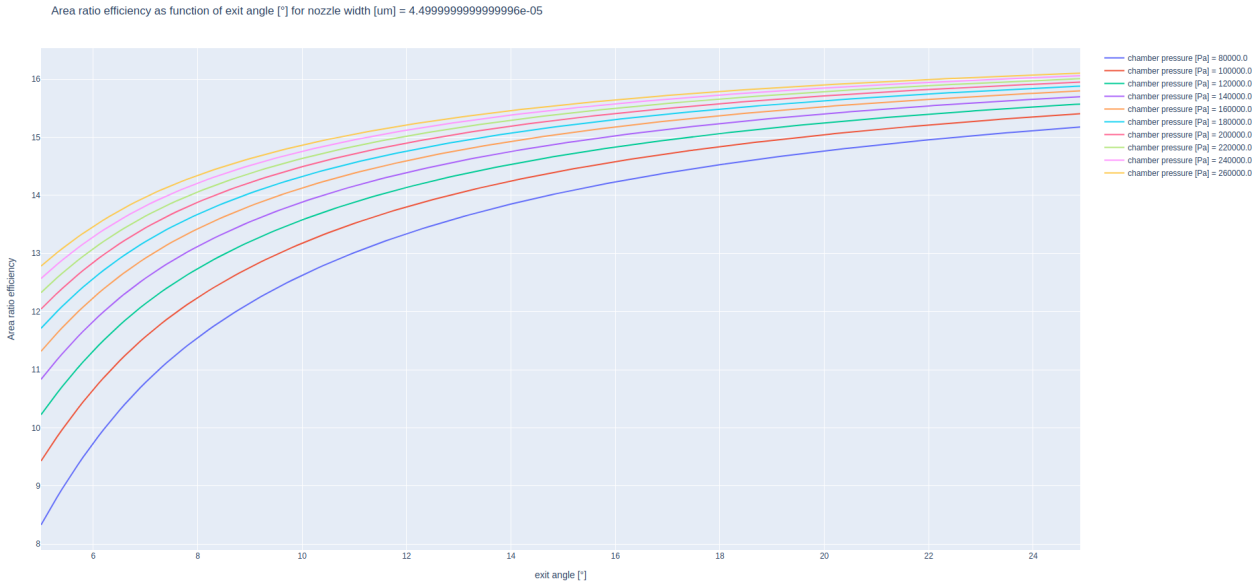

Figure 3: True area ratio as function of divergence angle

In order to see how different parameters affect the same performance metric, a closer look is taken at the specific impulse. At first, the divergence angle is ranged from 5 to 25 degrees. We see that, similarly to the thrust efficiency, the optimal is found for higher chamber pressures and lower exit angles:

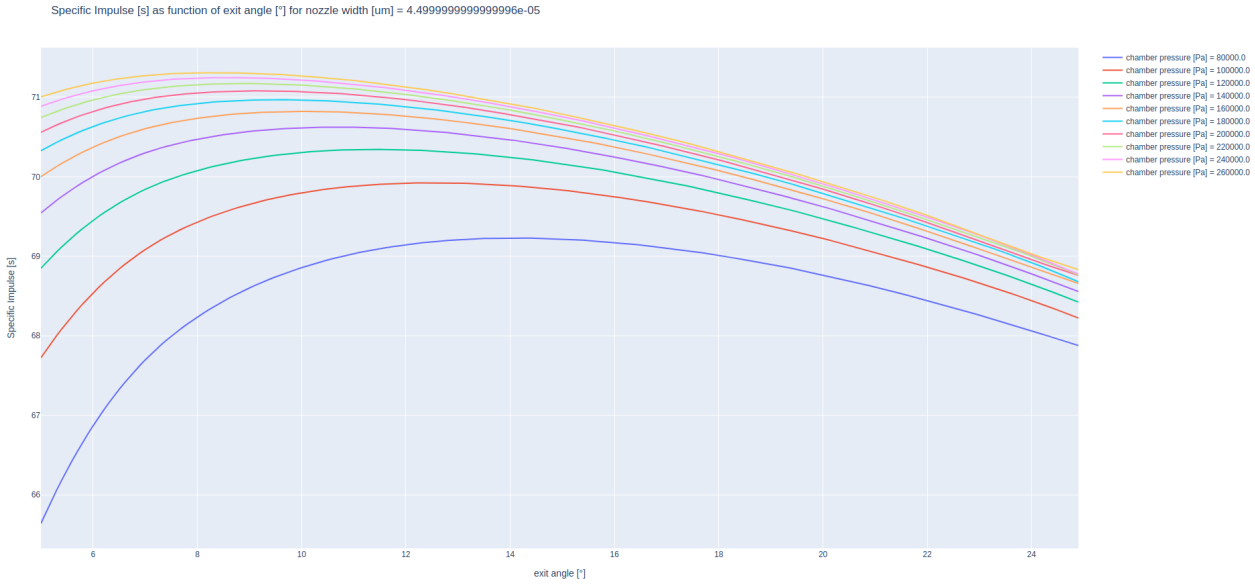

Figure 4: Specific Impulse as function of divergence angle

Next, the plot settings are changed. The x-axis variable is switched to 1 (throat width), and the plot variable is switched to 0 (exit angle). This means that the divergence angle will be kept constant in a single plot. The throat width is then varied from $40\mu m$ to $190\mu m$, resulting in the following plot:

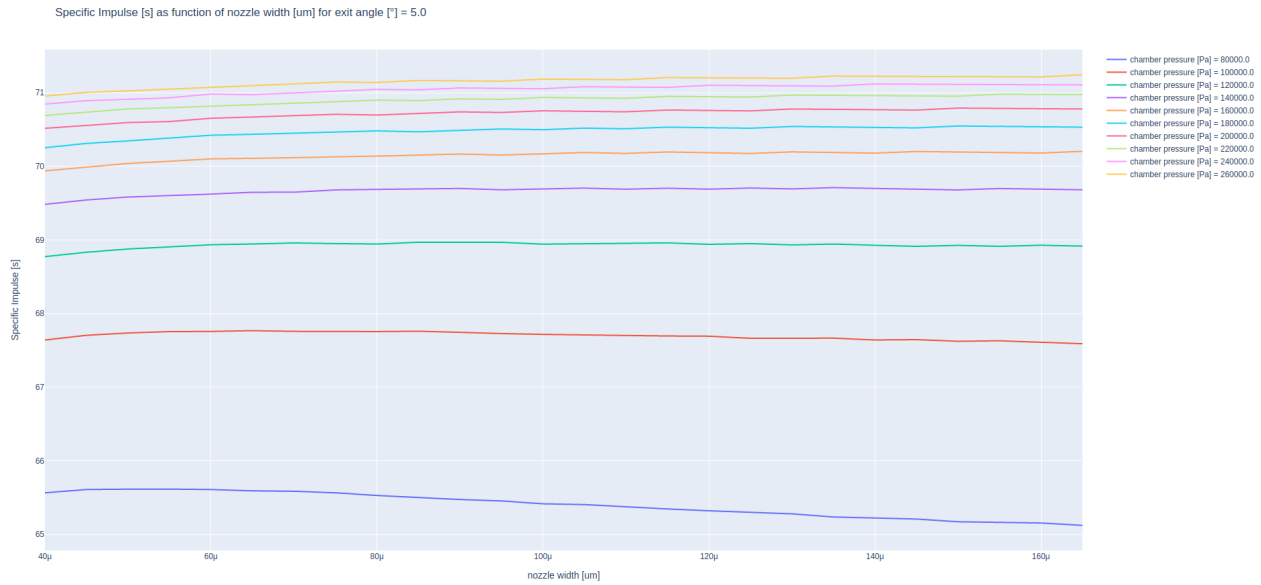

Figure 5: Specific Impulse as function of throat width

This curve shows that for chamber pressures above 2 bar, an increase in throat width results in an increased specific impulse (although the change is rather small). However, below this chamber pressure it appears that further increasing the throat width actually results in a decreased specific impulse. Further changing the plot settings to show how the chamber pressure influences specific impulse, we find the following relation:

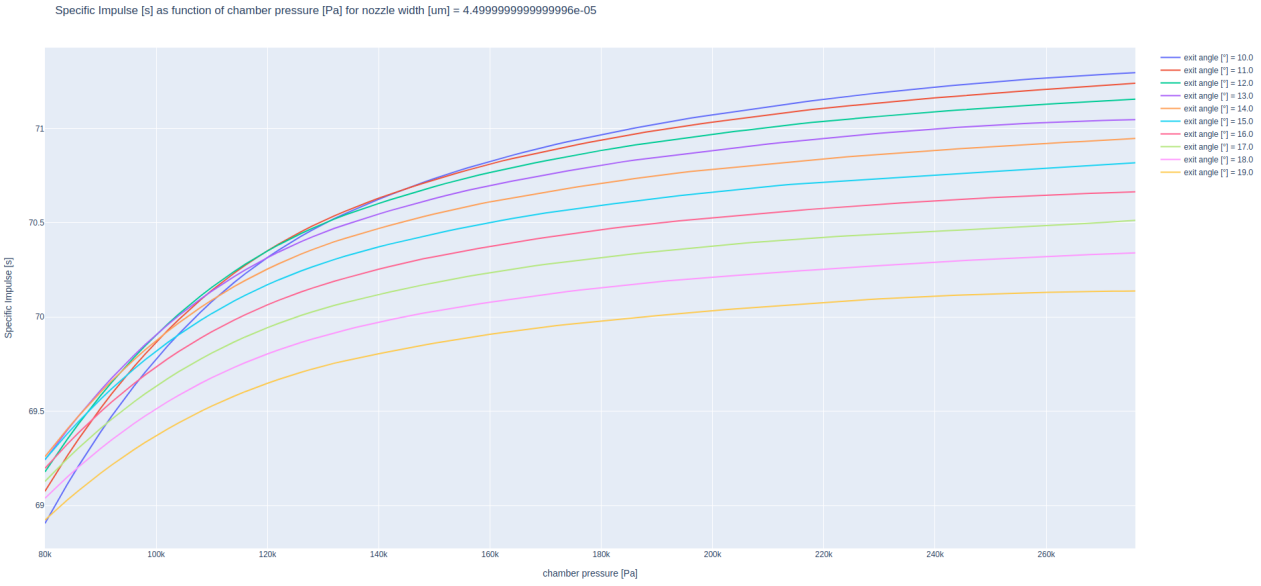

Figure 6: Specific Impulse as function of chamber pressure

Generally speaking, the specific impulse increases with chamber pressure. However it is interesting to note that for the lower pressure regimes (below 1.5 bar), the divergence angle resulting in the highest specific impulse is quite variate. For higher pressures though, it is clear that lower divergence angles increase the specific impulse. The various plots discussed in this section show a general trend in how performance changes when changing certain parameters. To a certain extent higher chamber pressures and lower exit angles tend to increase the nozzle performance and minimize losses. In order to settle on one set of design parameters, the design priorities must first be examined. If the objective is to maximize the thrust coefficient, this analytical analysis suggests selecting a chamber pressure of 2.2 bar and an exit angle of 9 degrees. However, the specific details of this configuration are dependent on more than the optimization of just one performance metric. section 4 discusses in more detail what elements would have to be added to this analysis in order to make a more definitive design choice.

4 Recommendations

The approach presented in this report has made a number of simplifying assumptions. This chapter provides an overview of these assumptions, and why they were deemed appropriate. In addition, recommendations are made on how the analytic prediction of micro-nozzle performance could be improved.

The assumption at the root of this analysis is the idea that the boundary layer development in a linear converging-diverging nozzle can be represented with flat plate boundary layer solutions for incompressible, laminar flow. Since the nozzle divergent is linear, and the Reynolds numbers in consideration are low, this was deemed an acceptable assumption for a simplified analysis. However, this assumption has several consequences. Most importantly, the boundary layer is assumed to begin its development at the throat. This means that the effective throat diameter itself, and thus also the discharge coefficient, remain unchanged. In reality, the boundary condition actually begins developing before reaching the throat. However, simplified solutions to boundary layer characteristics in a linear micro-nozzle are not readily available. An in-depth CFD analysis focused on determining simplified relations for boundary layer characteristics in such nozzles would allow this analytic method to be more accurate.

The second enabling assumption of this analytic approach is the idea that compressibility effects on the skin friction coefficient can be represented using the "Reference Temperature Approach". Again, a more in-depth study should be made to assess the applicability of this approach to micro-nozzles specifically.

Finally, assumptions were made on the wall temperature used in the Reference Temperature Approach. The true wall temperature is not a steady state parameter from the start of a burn. It will most likely go through a transient phase during start-up (during which efficiency will thus be different from steady state efficiency), before reaching a steady state temperature. This steady state temperature depends not only on flow conditions, but also on nozzle thermal mass and conductive/radiative environment. To accurately predict this more information would be required on the materials used for production.

The results presented in section 3 conclude that at present, the analytic approach underestimates the performance predicted by the numerical approach in [1] . The true performance of the nozzle can be obtained through testing only, but it is likely that the simplifying assumptions are at the cause of these discrepancies. Ideally, the simplifying assumptions made in this report would be replaced by more accurate relations by performing a CFD analysis dedicated to the matter.

5 Conclusion

This report presented a simplified approach to determining the effects a low Reynolds number has on nozzle efficiency. Specifically, flat plate boundary layer theory was combined with the "Reference Temperature Approach" to formulate an expression for the true thrust efficiency obtained from a micro-nozzle. The results of the approach appear to be underestimating performance when compared to the numerical analysis performed in [1]. Nevertheless, the approach has shown how the divergence angle of a linear convergent-divergent micro-nozzle affects performance for different Reynolds numbers. It was shown that low Reynolds numbers are much more susceptible to losses caused by boundary layers, while divergence losses dominate the higher Reynolds number cases. In order to further improve on this analytic approach, it would be desirable to perform a CFD analysis focused on assessing the development of the boundary layers in small nozzles. Such an analysis could allow for an analytic solution of boundary layer characteristics to be developed, that would be specific to micro-nozzles and low Reynolds number flow.

References

Ganani, C. S. (2019). *Micronozzle performance.* TU Delft.

H, S. (1979). *Boundary layer theory.* McGraw-Hill.

Zandbergen, B. T. C. (2018). *Thermal rocket propulsion.* TU Delft.